OXFORD

International Journal of Neuropsychopharmacology (2018) 21(3): 291–304

doi:10.1093/ijnp/pyx115
Advance Access Publication: December 8, 2017
Regular Research Article

REGULAR RESEARCH ARTICLE

Mitochondria Are Critical for BDNF-Mediated Synaptic and Vascular Plasticity of Hippocampus following Repeated Electroconvulsive Seizures

Fenghua Chen, Maryam Ardalan, Betina Elfving, Gregers Wegener, Torsten M. Madsen, Jens R. Nyengaard

Core Center for Molecular Morphology, Section for Stereology and Microscopy, Department of Clinical Medicine, Aarhus University, Aarhus, Denmark (Drs Chen and Nyengaard); Translational Neuropsychiatry Unit, Department of Clinical Medicine, Aarhus University, Risskov, Denmark (Drs Ardalan, Elfving, and Wegener); Centre for Stochastic Geometry and Advanced Bioimaging, Aarhus University, Aarhus, Denmark (Dr Nyengaard); Aptinyx Inc, Evanston, Illinois (Dr Madsen); Center of Excellence for Pharmaceutical Sciences, North-West University, Potchefstroom, South Africa (Dr Ardalan); Department of Clinical Medicine, Center of Functionally Integrative Neuroscience, Aarhus University, Aarhus, Denmark (Dr Ardalan); AUGUST Centre, Department of Clinical Medicine, Aarhus University, Risskov, Denmark (Dr Wegener).

Correspondence: Fenghua Chen, MD, PhD, Department of Clinical Medicine, Translational Neuropsychiatry Unit, Skovagervej 2, building 14K, 0.15, 8240 Risskov, Denmark (fenghua.chen@clin.au.dk).

Abstract

Background: Electroconvulsive therapy is a fast-acting and efficient treatment of depression used in the clinic. The underlying mechanism of its therapeutic effect is still unclear. However, recovery of synaptic connections and synaptic remodeling is thought to play a critical role for the clinical efficacy obtained from a rapid antidepressant response. Here, we investigated the relationship between synaptic changes and concomitant nonneuronal changes in microvasculature and mitochondria and its relationship to brain-derived neurotrophic factor level changes after repeated electroconvulsive seizures, an animal model of electroconvulsive therapy.

Methods: Electroconvulsive seizures or sham treatment was given daily for 10 days to rats displaying a genetically driven phenotype modelling clinical depression: the Flinders Sensitive and Resistant Line rats. Stereological principles were employed to quantify numbers of synapses and mitochondria, and the length of microvessels in the hippocampus. The brain-derived neurotrophic factor protein levels were quantified with immunohistochemistry.

Results: In untreated controls, a lower number of synapses and mitochondria was accompanied by shorter microvessels of the hippocampus in "depressive" phenotype (Flinders Sensitive Line) compared with the "nondepressed" phenotype (Flinders Resistant Line). Electroconvulsive seizure administration significantly increased the number of synapses and mitochondria, and length of microvessels both in Flinders Sensitive Line-electroconvulsive seizures and Flinders Resistant Line-electroconvulsive seizures rats. In addition, the amount of brain-derived neurotrophic factor protein was significantly increased in Flinders Sensitive Line and Flinders Resistant Line rats after electroconvulsive seizures. Furthermore, there was a significant positive correlation between brain-derived neurotrophic factor level and mitochondria/synapses.

Received: June 16, 2017; **Revised:** November 25, 2017; **Accepted:** December 5, 2017

Significance Statement

Synaptic transmission is the main energy-consuming process in the brain, and in addition synthesis of new neuropil (such as synaptogenesis and neurogenesis) imposes additional metabolic demands. Therefore, changes in mitochondrial and microvascular support might be expected in association with changes in neuropil. Moreover, BDNF is a well-known neurotrophic factor with a critical function in neuronal plasticity and regulation of mitochondrial transport and distribution. However, little is known about the role of mitochondrial and vascular changes and its relationship to synaptic plasticity. In the present study, we investigated whether synaptic plasticity induced by repeated ECS, a model for the clinically validated seizure treatment, is associated with enhanced metabolic activity by morphological alterations of the microvessels and mitochondria accompanied by BDNF level elevation.

Conclusion: Our results indicate that rapid and efficient therapeutic effect of electroconvulsive seizures may be related to synaptic plasticity, accompanied by brain-derived neurotrophic factor protein level elevation and mitochondrial and vascular support.

Keywords: synapse, mitochondria, microvessels, BDNF, ECS

Introduction

Electroconvulsive therapy (ECT), with the corresponding animal model electroconvulsive seizures (ECS), is a fast-acting and efficient treatment of depression used in the clinic (Ren et al., 2014). However, the underlying mechanism of its therapeutic effect is still poorly understood. Recent studies suggest that recovery of synaptic connections and synaptic remodeling is critical for the clinical efficacy obtained from a rapid antidepressant response and is not mediated entirely via neurogenesis (Li et al., 2010a, 2011; Kang et al., 2012). Growing evidence suggests that disruption of synaptic plasticity results in destabilization and loss of synaptic connections in depression (Popoli et al., 2002; Duman, 2004; Ardalan et al., 2017; Vose and Stanton, 2017). Animal studies have demonstrated changes in synapse type and number after antidepressant treatment in hippocampus (Chen et al., 2008, 2009, 2010; Hajszan et al., 2009a, 2010); Ardalan et al., 2017). Fluoxetine and S-ketamine induce rapid hippocampal synaptogenesis in the CA1 (Hajszan et al., 2009a; Ardalan et al., 2017), whereas onset of Dentate Gyrus (DG) neurogenesis often happens 3 to 4 weeks after treatment (Kodama et al., 2004; Marcussen et al., 2008).

A postmortem morphometric study has recently reported a decrease in the number of synapses in the dorsal lateral prefrontal cortex and a corresponding decrease in several synapse-related proteins in a small cohort of major depressive disorder (MDD) patients (Kang et al., 2012). However, any synthesis of new neuropil (such as synaptogenesis and neurogenesis) in these regions imposes additional metabolic demands, and synaptic transmission is the main energy-consuming process in the brain (Jonas, 2013; Obashi and Okabe, 2013). Therefore, some corresponding changes in mitochondrial and microvascular support might be expected in association with changes in neuropil. Moreover, brain-derived neurotrophic factor (BDNF) is a well-known neurotrophic factor with a critical function for neuronal plasticity and regulation of mitochondrial transport and distribution (Yoshii and Constantine-Paton, 2010; Su et al., 2014a) and therefore, changes in BDNF could also be possible.

Mitochondria play important roles in controlling fundamental processes of neuroplasticity (Mattson et al., 1999, 2008; Ruthel and Hollenbeck, 2003), and altered mitochondrial function has been implicated in alterations of synaptic plasticity (MacAskill et al., 2010; Sun et al., 2013). Growing evidence from electron microscopy, imaging, and genetic studies suggest that mitochondrial dysfunction and abnormal mitochondrial structure in neurons is implicated in psychiatric disorders (schizophrenia, bipolar disorder, and MDD) (Shao et al., 2008; Shao and Vawter, 2008; Scaglia, 2010; Cataldo et al., 2010; Chen et al., 2013). Vascular plasticity is another important structural mechanism regulating the replication, survival, and differentiation of cells. Impairments of vascular plasticity of the hippocampus have been shown in hippocampal subregions in animal models of depression (Czeh et al., 2010; Ardalan et al., 2016, 2017), and, more interestingly, the counteracting effect of antidepressant treatment on vascular plasticity of hippocampus has been observed (Newton et al., 2006; Ardalan et al., 2016). Furthermore, research has revealed that the brain-specific angiogenesis inhibitor plays an important role in synaptogenesis and/or function (Duman et al., 2013; Stephenson et al., 2013). Moreover, one postmortem study supports the hypothesis that antidepressants increase human hippocampal angiogenesis (Boldrini et al., 2012).

This study was designed to test the hypothesis that the mechanism underlying rapid antidepressant effect of ECS in a genetic animal model of depression, the Flinders Sensitive Line (FSL) and their controls, the Flinders Resistant Line (FRL) rats (Overstreet et al., 2005), is integrating synaptic plasticity and nonneuronal plasticity (vascular and mitochondria). It can be speculated that synaptic plasticity is associated with enhanced metabolic activity by morphological alterations of the microvessels and mitochondria accompanied by BDNF level elevation.

Materials and Methods

The treatment and preparation of the tissue has been presented elsewhere (Kaae et al., 2012).

Animals

Adult male FSL (n = 12, 6/ECS, 6/sham) and FRL (n = 12, 6/ECS, 6/sham) rats (180–200 g) from breeding colonies maintained in the animal quarters of Translational Neuropsychiatry Unit, Aarhus University Hospital were kept on a normal 12-hour-light/-dark cycle and had free access to food and water. The study protocol was approved by the Danish animal ethics committee (approval no. 2007/561–1378).

Animals were treated once daily for 10 days every day at 9 AM. ECS was given via ear clip electrodes using 55 to 70 mA

in 0.5 seconds at a frequency of 100 Hz square wave pulses (UgoBasile). All ECS-treated rats were monitored for seizures ensuring that clonic movements of the face and forelimbs lasted for at least 10 seconds. The sham-treated group was exposed to the same procedure without current passed. The behavioral assessment in the porsolt swim test (Porsolt et al., 1978) of the animals investigated has been reported elsewhere (Kaae et al., 2012). Despite a recent study showing that the methodological application of ECS applied in the current work needs to be refined and may result in microfractures in the skeletal system of the animals (Ekemohn et al., 2017) due to omission of a muscular relaxant, the morphological and molecular findings in the present work should not be affected.

Tissue Preparation and Sampling

Rats were deeply anesthetized with pentobarbital sodium (Unikem A/S) and perfused transcardially by fixatives (4% paraformaldehyde and 2% glutaraldehyde) 15 hours after the last ECS or sham treatment. Hippocampi were isolated, and left or right hippocampus was selected randomly, embedded in 5% agar, and sectioned at 65-µm thickness on a Vibratome 3000 (Vibratome). Three sets of sections were chosen based on a systematic random sampling principle and a section sampling fraction of 1/15. One set was stained with Thionin for estimating the volume of subregions of hippocampus and the length of blood vessels with light microscopy and another set was stained against BDNF using immunohistochemistry. The last set of tissue sections for electron microscopy was embedded in TAAB 812 Epon for cutting 20 consecutive serial ultrathin sections. The actual mean ultrathin section thickness (69–72 nm) was determined according to Small's method of minimal folds (Small, 1968). Electron micrographs were taken with a digital camera in a Philips CM 10 electron microscope at an initial magnification of 10500× and digitally enlarged to a final magnification of 23850×. The micrographs were saved and later analyzed via iTEM software (Olympus Soft Imaging Solutions) without any postprocessing modifications.

Synapse and Mitochondria Counting

We used the physical disector (Sterio, 1984), which was modified from previous studies (Tang et al., 2001) for estimating synapse and mitochondria number. The synapses were identified primarily based on the presence of a postsynaptic density (PSD) with vesicles in proximity to the presynaptic zone. Only spine and shaft synapses of asymmetric synapses were analyzed in this study. The spine synapses presented a clear cytoplasmic matrix and a distinct spine apparatus but without mitochondria and microtubules. The shaft synapses terminated directly on the dendritic shaft. The dendrites were differentiated from spines by a less densely stained cytoplasm containing microtubules and mitochondria. The spine synapses may be subdivided into perforated and nonperforated synapses. Perforated synapses displayed discontinuous or perforated PSD profiles, whereas nonperforated synapses exhibited continuous PSD files in all consecutive sections (Figure 1) (Geinisman et al., 2001).

The synapse number density was estimated using the PSD as a counting unit. Axo-spinouos perforated synapses and shaft synapses were counted with ~120 disectors and axo-spinous nonperforated synapses with ~48 disectors in each animal. The total synapse number was estimated as the product of the synapse number density and volume of the CA1 stratum radiatum (CA1-SR). We used the Cavalieri estimator and 2D nucleator combined for quantifying the volume of hippocampus on one set of sections stained with Thionin using a 4× lens (Dorph-Petersen et al., 2001). Detailed information can be found in our previous paper (Chen et al., 2010).

Mitochondria were counted throughout the neuropil and specifically in the axon terminals and dendrites. The criteria for identifying mitochondria were the presence of distinctive cristae and a double membrane (Figure 1). Neuropil structures were identified as axon terminals (presence of three or more synaptic vesicles), dendrites (postsynaptic to a synapse or having an attached spine), or astroglial processes (presence of fibrils and watery cytoplasm). The total number of mitochondria in neuropil and the number of mitochondria in axon terminals and dendrites were determined.

Combining the disector principle with the object's 3D Euler number estimates the number of mitochondria (Kroustrup and Gundersen, 2001). The total Euler number, Σx, contribution from all disectors is obtained as the signed sum of islands and bridges (Figure 1). The total mitochondria number was estimated as the product of the mitochondria number density and volume of CA1-SR. Detailed information can be found in our previous paper (Chen et al., 2013).

Estimation of the Length Density and Total Length of Microvessels

Measurement of length density and total length of the microvessels in CA1-SR was done by implementation of the global spatial sampling method (Larsen et al., 1998). The microvessel was defined as a vessel with a 1-celled wall and a diameter ≤10 µm.

The microvessel length was measured with a 60× oil immersion lens (Olympus, Plan Apochromat, N.A. 1.35). Within 3-dimensional sampling box, the distance between isotropic virtual planes was (d = 25 µm) and systematically and randomly projected on the area of interest. The estimation of the length density of the microvessels was done by counting the total number of intersections between the virtual planes and the microvessels (Figure 2A). The total length of the microvessels was calculated by the length density of the microvessels multiplied by volume of CA1-SR. Detailed information can be found in our previous paper (Ardalan et al., 2016).

Immunohistochemistry

Free-floating 8 to 9 coronal sections per animal were washed 3 times for 10 minutes in Tris-buffered saline (TBS) (pH 7.4), immersed in endogenous peroxidase blocking solution for 30 minutes, and incubated in preheated Target Retrieval solution at 85°C for 40 minutes (Dako, EnVision System HRP). Tissue sections were incubated at 4°C overnight in a solution containing the rabbit anti-BDNF polyclonal antibody (diluted 1: 500) (AB1779, Merck Millipore). Then, sections were washed 3 times for 10 minutes with buffer (1% BSA and 0.3% Triton-X in TBS) and incubated in buffer (1% BSA in TBS) added goat anti-rabbit IgG (1:200) for 2 hours at room temperature. Finally, sections were washed 3 times for 10 minutes in TBS and then visualized with 0.1% 3, 3'-diaminobenzidine containing 0.3% H_2O_2 in TBS for 7 minutes and washed by TBS 3 times for 10 minutes. Sections were then mounted on the gelatin-coated slides and dehydrated with alcohol gradient and cleared with xylene.

Images of immunostained sections were taken using an Olympus BX61VS Scan microscope (objective: 10X; Olympus) equipped with a PIKE digital camera using the software VS ASW OIL 2.7 (Olympus Soft Imaging Solutions GmbH). ImageJ software

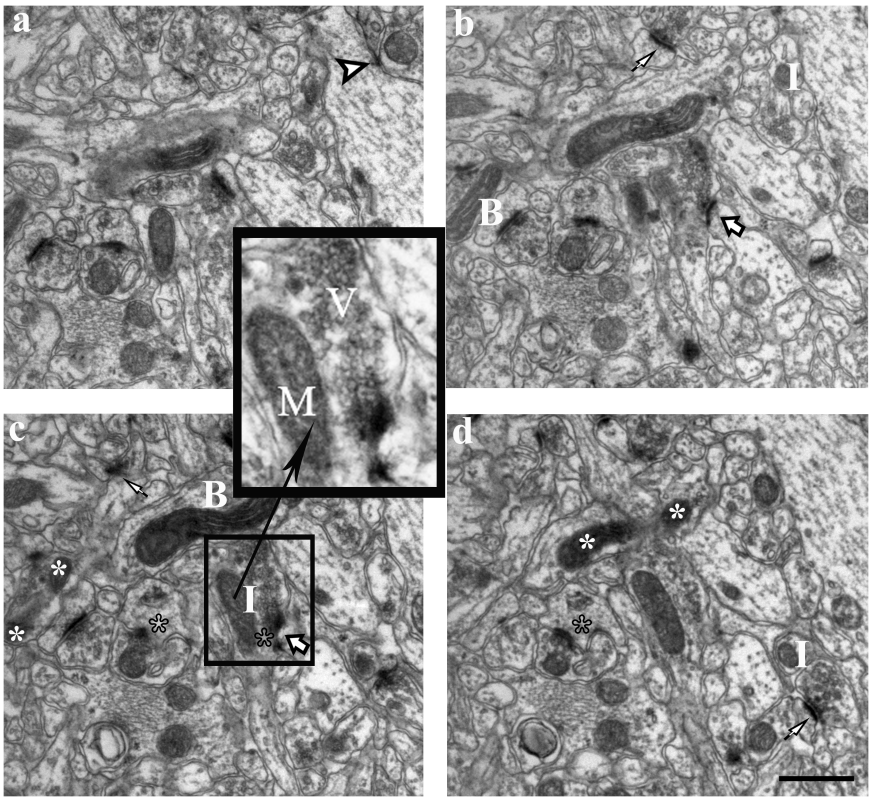

Figure 1. Estimation of synapses and mitochondria in consecutive serial sections, inserted survey with details (boxed areas). The synapses were identified primarily based on the presence of a postsynaptic density (PSD) with vesicles in close proximity to the presynaptic zone. Electron micrographs of consecutive ultrathin sections (a–d) showed nonperforated synapses (arrows), a perforated synapse (big arrows), and shaft synapse (arrow heads). The postsynaptic spine exhibited PSD discontinuities (black stars). The criteria for identifying mitochondria were the presence of distinctive cristae and a double membrane. Axon terminals were identified as presence of 3 or more synaptic vesicles. Dendrites were identified postsynaptic to a synapse or having an attached spine. Mitochondria are identified in each section plane, and a change between planes is deduced as being 1 of 2 significant possibilities: a new isolated part, a so-called "Island," I, or a new connection between isolated mitochondria, a "Bridge", B. Mitochonria (M); vesicles (V); branch dividing (white stars). Scale bar, 0.5 μm.

was used to analyze the images of immunostained sections and calculated the mean optical density of BDNF-positive area in subregions (DG, CA1, and CA2/3) of hippocampus (Figure 3).

Statistical Procedures

All data in FSL/FRL rats were subjected to 2-way (with 2 factors: strain and treatment) ANOVA to compare treatment responses following posthoc tests (Bonferroni and least significant difference). $P < .05$ was considered statistically significant. Correlations between parameters were analyzed by Pearson correlation coefficient. Statistical analyses and graphical representations of the findings were carried out using SPSS11 (SPSS Corp.) and Sigmaplot 10 (SYSTAT Inc.) software. The coefficient of error for the sampling protocol used in the present study ranged from 0.031 to 0.046; the coefficient of error was less than one-half the CV (0.064 to 0.157). This indicated that the major contributor of the group variance was the biological variability among the rats, rather than the sampling precision of each estimate. In other words, the sampling parameters utilized in this study were at an appropriate level of precision (Table 1).

Results

The Volume of Hippocampal CA1-SR

The volume of hippocampal CA1-SR in the FRL sham rats was significantly larger compared with the FSL sham group ($P < .05$). After ECS treatment, the volume of hippocampal CA1-SR in the FSL-ECS group was significantly increased compared with the FSL sham group ($P < .05$) (Figure 4).

The Number of Synapses in Serial Sections

In the sham-treated FSL group, the number of total synapses ($F_{1, 20} = 9.61$; $P < .01$), nonperforated synapses ($F_{1, 20} = 15.59$; $P < .01$), and perforated synapses ($F_{1, 20} = 3.41$; $P < .05$) in CA1-SR was significantly lower compared with the sham-treated FRL group.

In FRL rats, ECS treatment significantly increased the number of nonperforated spine synapses ($P < .05$ vs FRL-sham) (Figure 5B). However, no changes of total number of synapses were observed. In FSL rats, the nonperforated, perforated spine and total synapse numbers significantly increased in ECS treated rats ($P < .01$, $P < .01$, and $P < .01$, respectively, vs FSL sham) (Figure 5A–C). Conversely, the shaft synapse number decreased significantly in both FRL-ECS and FSL-ECS rats ($P < .05$) (Figure 5D).

The Number of Mitochondria in Serial Sections

Mitochondria are dynamically transported in and out of axons and dendrites to maintain neuronal and synaptic function. Therefore, we wanted to investigate whether the number of mitochondria differs in axons and dendrites. In axon terminals and total neuropil, the mitochondria number was significantly lower in the FSL sham group compared with the FRL sham

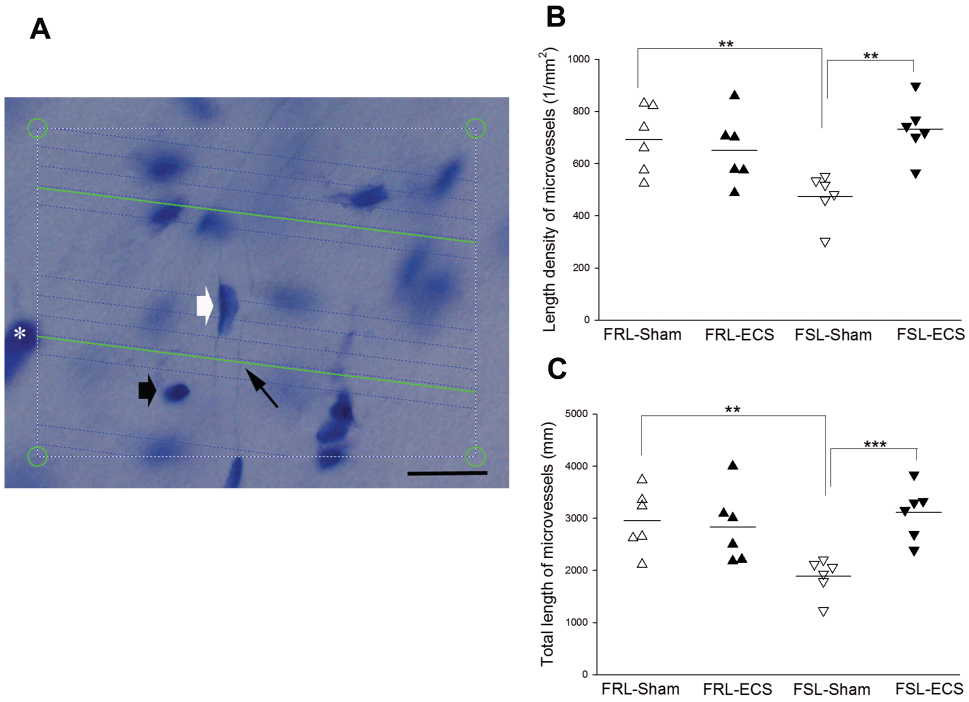

Figure 2. (A) The length of microvessels was measured within a 3-dimensional sampling box. Green test lines were superimposed on the live image by newCAST software, and they represented the intersection between isotropic virtual planes intersect and the focal plane. Microvessel is defined as a vessel with a 1-celled wall and endothelial cells lining blood vessel walls and a diameter ≤10 µm. The sampling box area was 7200 µm^2 and the box height was 20 µm. When the microvessels are in focus and virtual planes intersect them, they are counted. The 4 box corner points are used to estimate the reference volume. One microvessel is intersecting a green line of virtual plane (small black arrow). Pyramidal cell (*), glial cell (black thick arrow) and endothelial cell (white thick arrow). (B–C) Effect of electroconvulsive seizures (ECS) on hippocampal vascular plasticity: length of microvessels. (**P < .01) (ΔFlinders Resistant Line (FRL)-Sham rats; ▲FRL-ECS rats; ▽Flinders Sensitive Line (FSL)-Sham rats; ▼FSL-ECS rats). The length density (B) and the total length (C) of the microvessels in the CA1.SR were significantly higher in FRL-sham rats compared with FSL-sham. ECS treatment significantly increased both the length density (B) and the total length (C) of the microvessels in the CA1.SR in FSL rats.

group ($F_{1, 20}$ =9.02; P<.01 and $F_{1, 20}$=10.68; P<.001) (Figure 6A–B). However, there was no significant difference in the dendrites mitochondria number between FSL sham and FRL sham groups (P>.05) (Figure 6C). In the FSL group, ECS treatment significantly increased the mitochondria number in axon terminal and total neuropil, but not in dendrites ($F_{1, 20}$ =29.5; P<.001 and $F_{1, 20}$=23.18; P<.001) (Figure 6A–C).

Mitochondria Volume

The volume of mitochondria is shown in Figure 6D. A significantly larger volume was found in the FSL sham group compared with the FRL sham group (P<.001). After ECS treatment, the mitochondrial volume was significantly decreased in the ECS treated FSL group compared with the FSL sham group (P<.001). Two-way ANOVA analysis showed that the volume of mitochondria in CA1 area was significantly influenced by strain ($F_{1, 20}$ =14.61; P<.01) and treatment ($F_{1, 20}$ =29.81; P<.001) with a significant strain × treatment interaction ($F_{1, 20}$=18.13; P<.001).

The Effect of ECS on the Length of the Microvessels in CA1 Stratum Radiatum

The results of microvessel length density in the CA1.SR area of hippocampus showed a significant strain × treatment interaction ($F_{1, 20}$=9,99; P<.01). The length density of microvessels was significantly smaller in FSL-sham rats than the FRL-sham group (P<.05). The evaluation of the effect of the ECS on the length density of hippocampal microvessels showed that ECS treatment significantly (P<.01) increased length density of microvessels in FSL rats, while this difference was not significant in FRL group (Figure 2B).

Regarding the plasticity of total length of hippocampal microvessels, a 2-way ANOVA revealed the effect of treatment ($F_{1, 20}$=6.05; P<.05) and interaction between ECS treatment and strain ($F_{1, 20}$=8.95; P<.01). The total length of the microvessels was significantly higher in FRL-sham rats compared with FSL-sham (P<.05) (Figure 2C). Furthermore, ECS treatment affected significantly the total length of microvessels in FSL rats (P<.01) but not the FRL rats.

Hippocampus BDNF Expression Levels by Immunohistochemistry

BDNF positive immunoreactivity was mainly localized in the intracytoplasm of neurons. Mean optical density (MOD) of BDNF in DG (P<.01), CA2/3 (P<.05), and CA1 (P<.05) of hippocampus was significantly higher in both FSL and FRL rats after ECS treatment compared with the sham rats (Figure 3). Two-way ANOVA analysis showed that the MOD of BDNF in DG ($F_{1, 20}$=201.92; P<.01), CA2/3 ($F_{1, 20}$=219.81; P<.01), and CA1 ($F_{1, 20}$=260.19; P<.01) was significantly influenced by treatment. However, there was no difference between the FRL-sham and FSL-sham rats.

Correlations between Synapse, Mitochondria, Vascular Plasticity, and BDNF Level in the Hippocampus Following ECS Treatment

In Figure 7 correlations of morphological data and BDNF values are given. The levels of BDNF were positively correlated with

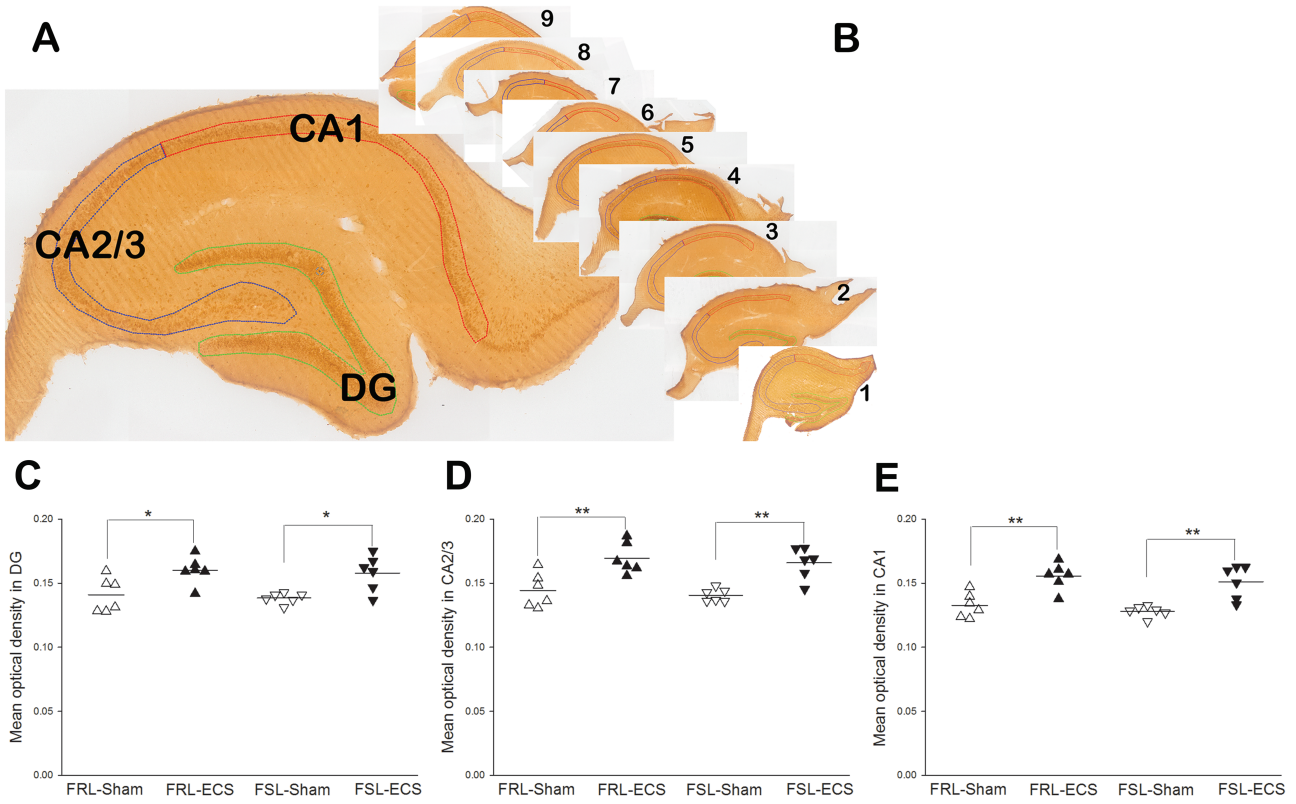

Figure 3. Brain-derived neurotrophic factor (BDNF) expression levels were measured by immunohistochemistry in hippocampus. (A) BDNF expression in the subregions of hippocampus. (B) BDNF expression in serial sections of hippocampus in each animal. (B–D) Immunohistochemistry examined BDNF expression levels in each group. Mean optical density (MOD) was calculated with the following formula: OD = log10 (max pixel intensity/mean pixel intensity), where max pixel intensity = 255. MOD in the electroconvulsive seizures (ECS)-treated group significantly increased compared with sham group in both Flinders Resistant Line (FRL) and Flinders Sensitive Line (FSL) rats in DG (B), CA2/3 (C), and CA1 (D) subregions of hippocampus.

synapse number ($r = 0.46$; $P < .05$) and mitochondrial number ($r = 0.55$; $P < .01$) but not with the total length of microvessels. The total length of microvessels showed a significant positive correlation with synapse number ($r = 0.64$; $P < .01$) and mitochondrial number ($r = 0.68$; $P < .001$). In addition, the volume of hippocampal CA1-SR was significant positively correlated with synapse number ($r = 0.69$; $P < .001$), mitochondrial number ($r = 0.71$; $P < .001$), and total length of microvessels ($r = 0.62$; $P < .01$). Furthermore, there was a significant positive correlation between the total mitochondria number and total number of synapses ($r = 0.77$; $P < .001$).

Discussion

Neuronal and nonneuronal plasticity play important roles in neurological disorders (Dong and Greenough, 2004). Recently, it was demonstrated that synaptic plasticity is disrupted in MDD, and antidepressant treatment produced opposing effects (Pittenger and Duman, 2008). However, little is known about the role of nonneuronal plasticity, especially mitochondrial and vascular plasticity, and the relationship of synaptic plasticity and nonneuronal plasticity in depression. In the present study, we report a lower number of synapses and mitochondria accompanied by a decreased length of microvessels in the "depressive-like" (FSL) rats compared with the FRL rats. For the first time, quantitative mitochondrial differences have been shown between axons and dendrites in a rat model of depression. In addition, we demonstrated that ECS has stimulative effect on the number of synapses and mitochondria and length of microvessels. Interestingly, the changes of mitochondrial number only happened in the axons and not in dendrites after ECS treatment in "depressive-like" rats. Furthermore, this study firstly showed that increased total synapse number is positively correlated with total mitochondria number, vascular total length, and BDNF. This result supports the hypothesis that synaptic plasticity needs enhanced metabolic activity by increased mitochondria number and length of microvessels.

A recent study showed that the methodological application of ECS applied in the current work may result in microfractures in the skeletal system of the animals (Ekemohn et al., 2017) due to omission of a muscular relaxant. Behavioral findings with the same methodology should therefore be treated with caution. The morphological and molecular findings in the present work should not be affected, and the changes in mitochondrial number are a consistent feature of neuroplasticity, emphasizing that the relation between synapses and mitochondria is a pivot for neuronal plasticity.

Effect of ECS on Hippocampal Synaptic Plasticity

Recent findings suggest that more rapid synaptic plasticity may play an important role in the neurobiology of depression and effects of antidepressant therapy (Popoli et al., 2002; Duman, 2004). In the present study, ECS treatment significantly increased the number of spine synapses, and, conversely, the shaft synapses decreased significantly in FRL and FSL rats. This increase was associated with an improvement in a behavioral readout in the forced swim test (Kaae et al., 2012). The present findings

Table 1. The overall measurement results of ultrastructure are summarized

			FRL-sham vs. FRL-ECS		
	FRL-sham	FRL-ECS	OCV	OCE	P
$V_{(CA1)}$ mm^3	4.25 (0.22)	4.33 (0.25)	0.06	0.04	.53
Total N(syn/CA1) $x10^9$	9.19 (0.96)	9.88 (0.91)	0.15	0.04	.34
N(np-syn) $x10^9$	6.28 (0.48)	7.14 (0.42)			< .05*
N(p-syn) $x10^9$	2.34 (0.45)	2.37 (0.55)			.92
N(sh-syn) $x10^9$	0.57 (0.07)	0.37 (0.07)			< .05*
Total N(mit/CA1) $x10^9$	5.01 (0.58)	5.38 (0.44)	0.10	0.05	.27
N(a-mit) $x10^9$	2.49 (0.51)	2.84 (0.34)			.16
N(d-mit) $x10^9$	1.34 (0.12)	1.56 (0.17)			.11
VN(mit/CA1) μm^3	0.05 (0.003)	0.49 (0.003)	0.06	0.03	.41
Total V(mit/CA1) mm^3	0.29 (0.03)	0.27 (0.02)			.87

			FSL-sham vs. FSL-ECS			FRL-sham vs. FSL-sham		
	FSL-sham	FSL-ECS	OCV	OCE	P	OCV	OCE	P
$V_{(CA1)}$ mm^3	3.98 (0.05)	4.27 (0.24)	0.07	0.04	< .05*	0.07	0.04	0.06
Total N(syn/CA1) $x10^9$	6.65 (1.21)	9.40 (1.03)	0.15	0.04	< .01**	0.15	0.04	< .01**
N(np-syn) $x10^9$	4.66 (0.79)	6.54 (0.93)			< .01**			< .01**
N(p-syn) $x10^9$	1.44 (0.34)	2.53 (0.45)			< .01**			< .05*
N(sh-syn) $x10^9$	0.55 (0.24)	0.34 (0.12)			< .05*			.79
Total N(mit/CA1) $x10^9$	3.53 (0.43)	5.37 (0.74)	0.13	0.04	< .001***	0.12	0.05	< .001***
N(a-mit) $x10^9$	1.40 (0.22)	2.90 (0.52)			< .001***			< .01**
N(d-mit) $x10^9$	1.46 (0.31)	1.34 (0.27)			.39			.36
VN(mit/CA1) μm^3	0.08 (0.01)	0.05 (0.008)	0.16	0.03	< .001***	0.11	0.03	< .001***
Total V(mit/CA1) mm^3	0.27 (0.02)	0.26 (0.01)			.39			.84

V(CA1): volume of CA1 stratum radiatum; N(syn/CA1): total number of synapses in CA1; N(np-syn): the number of non-perforated synapses; N(p-syn): the number of perforated synapses; N(sh-syn): the number of shaft synapses; N(mit/CA1): number of mitochondria in CA1; N(a-mit): the number of mitochondria in axons; N(d-mit): the number of mitochondria in dendrites; V_N(mit/CA1): mean volume of mitochondria; V(mit/CA1): total volume of mitochondria in CA1.

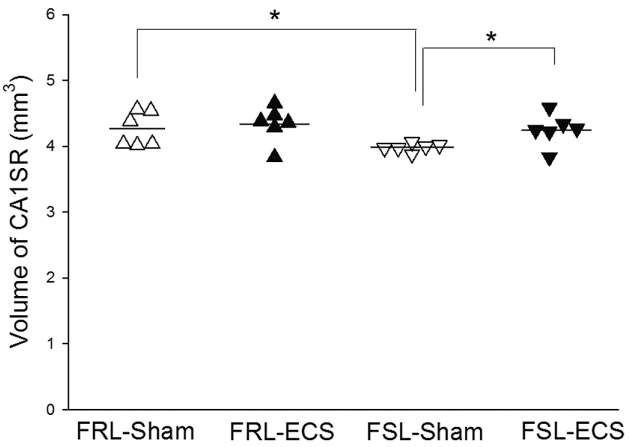

Figure 4. The volume of hippocampal CA1 stratum radium. The volume of hippocampal CA1-SR in the Flinders Resistant Line (FRL) sham rats is significantly larger than that of the Flinders Sensitive Line (FSL) sham group. After electroconvulsive seizure (ECS) treatment, the volume of hippocampal CA1-SR in the FSL-ECS group is significantly increased compared with the FSL sham group. (*P < .05) (ΔFRL-Sham rats; ▲FRL-ECS rats; ▽FSL-Sham rats; ▼FSL-ECS rats).

are consistent with imipramine significantly increasing synapse number in the FSL rats (Chen et al., 2010) and in another animal model of depression (Hajszan et al., 2005, 2009b).

In recent years, live imaging of developing dendrites demonstrated that a shaft synapse bouton can redistribute to contact an adjacent newly emerged dendritic spine (Reilly et al., 2011). Hippocampal synaptic plasticity following LTP induction showed a considerable restructuring of preexisting synapses, with shaft and stubby spines transforming to thin dendritic spines (Sorra et al., 1998; Popov et al., 2004; Bae et al., 2012). Our findings indicate that the changes of synapses may include both synaptogenesis and restructuring of existing synapses (shaft converting into spine synapses) to make them more efficient.

At the molecular level, perforated PSDs of synapses are typically larger and contain a greater number and concentration of receptors and/or cytoskeleton-associated proteins within the postsynaptic active zone than nonperforated spines (Nicholson and Geinisman, 2009). Our findings show that only the perforated spine synapses increased significantly in ECS treated FSL rats compared with sham treated FSL rats. Therefore, perforated spine synapses may have a more active function to enhance synaptic efficacy of synaptic transmission in the depressed status following antidepressant treatment. It has been hypothesized that changes in the configuration of synapses are critical for the synaptic plasticity, and perforated synapses, especially, are important for synaptic plasticity (Calverley and Jones, 1990; Geinisman et al., 2000; Toni et al., 2001; Ganeshina et al., 2004).

Effect of ECS on Hippocampal Mitochondrial Plasticity

Synaptic transmission requires mitochondrial ATP generation for neurotransmitter exocytosis, vesicle recruitment, activation of ion conductance, signaling at metabotropic receptors, potentiation of neurotransmitter release, and synaptic plasticity (Li et al., 2010b; Jiao and Li, 2011). Indeed, altered mitochondrial function has been implicated in alterations in synaptic plasticity (MacAskill and Kittler, 2010). Mitochondrial number and size are tightly regulated by balanced fusion and fission

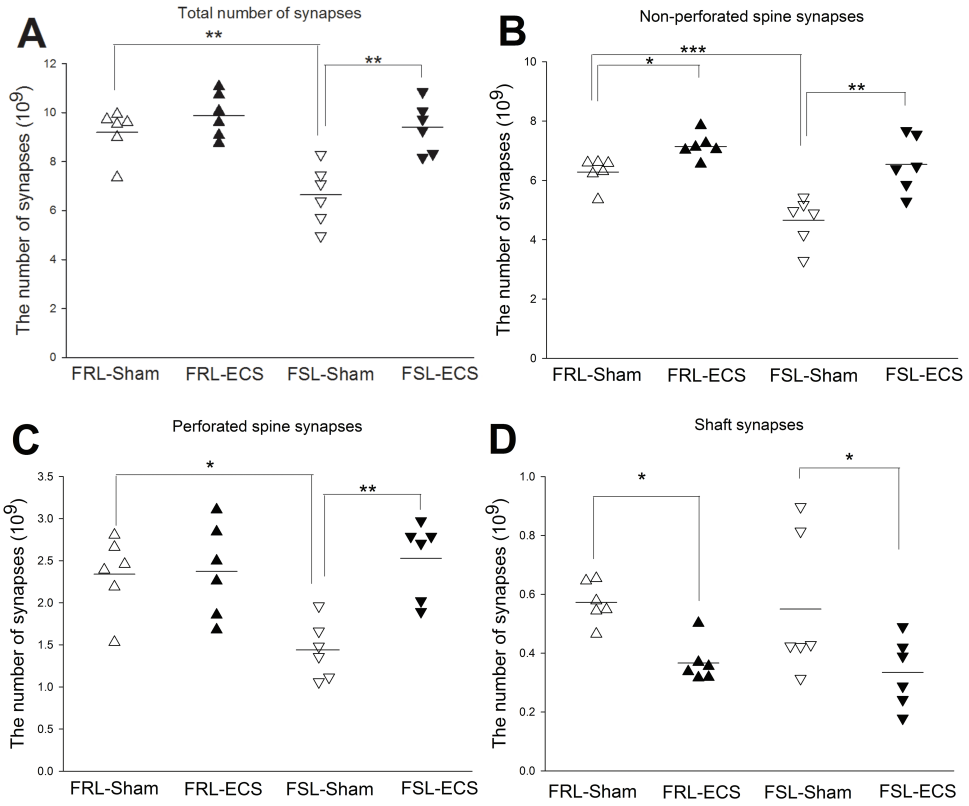

Figure 5. The number of synapses including subtypes of synapse in CA1 (*P < .05; **P < .01) (ΔFlinders Resistant Line (FRL)-Sham rats; ▲FRL-electroconvulsive seizure (ECS) rats; ▽Flinders Sensitive Line (FSL)-Sham rats; ▼FSL-ECS rats). (A) The total number of synapses was significantly higher in FRL-Sham rats compared with FSL-Sham rats. ECS treatment significantly increased the total number of synapses in FSL-ECS rats compared with FSL-sham rats. (B) The number of nonperforated spine synapses was significantly higher in FRL-Sham rats compared with FSL-Sham rats. ECS treatment significantly increased the number of nonperforated spine synapses in FRL-ECS rats compared with FRL-sham rats and FSL-ECS rats compared with FSL-sham rats. (C) The number of perforated spine synapses was significantly higher in FRL-Sham rats compared with FSL-Sham rats. ECS treatment significantly increased the number of perforated spine synapses in FSL-ECS rats compared with FSL-sham rats. (D) Conversely, ECS treatment significantly decreased the number of shaft synapses in FRL-ECS rats compared with FRL-sham rats and FSL-ECS rats compared with FSL-sham rats.

events in response to changes in the metabolic conditions of cell (Chan et al., 2006; Detmer and Chan, 2007; Cheng et al., 2010). Nevertheless, defects in mitochondrial fusion and fission primarily affect neuronal function; neurons are particularly sensitive to perturbations of mitochondrial distribution (Westermann, 2010). And this may contribute to the pathogenesis of neurodegenerative diseases and psychiatric disorders (Chen and Chan, 2009). Our findings indicate that changes in the mitochondrial number are consistent features of neurogenesis (Kaae et al., 2012) and synaptogenesis. Therefore, mitochondrial biogenesis may play an important role in the formation and maintenance of hippocampal synapses and may reflect alterations in neuronal activity associated with variation in abnormal energy demands related to major depression.

Mitochondria constantly move along axons and dendrites, dividing and fusing in response to synaptic changes and changing regional metabolic requirements (Mattson et al., 2008; Palmer et al., 2011). The correct mitochondrial distribution in axons and dendrites is closely related to the neuronal development, maintenance of axon and dendrites, and the formation of spines and synapses (Kang et al., 2008; van et al., 2013). The role and functional properties of mitochondria differ in axons (for the generation of action potentials and trafficking of synaptic vesicles) and dendrites (for synaptic transmission and extension/movement of mitochondria into dendritic protrusions) (Zinsmaier et al., 2009). Moreover, twice as many mitochondria are motile in the axons compared with the dendrites of cultured hippocampal neurons, and there is a greater proportion of highly charged, more metabolically active mitochondria in dendrites than in axons (Overly et al., 1996). Therefore, the difference in motility and metabolic properties of mitochondria in axons and dendrites reflects alterations in energy metabolism during synaptic plasticity. Our data show twice as many mitochondria in the axons compared with the dendrites in FRL rats. However, in the FSL rats, the number of mitochondria is equal in axons and dendrites. ECS treatment increases the mitochondrial number in axons twice the number of mitochondria in dendrites in FSL rats. Since most metabolic activity takes place in axon terminals (Zinsmaier et al., 2009), an increased number of mitochondria in axon terminals after ECS treatment in our study implies that the increased metabolism supports the generation of action potentials and trafficking of synaptic vesicles (neurotransmitter exocytosis and vesicle recruitment).

Elevated levels of glutamatergic neurotransmission have been observed in FSL rats (Matrisciano et al., 2008; Kovacevic et al., 2012; Gomez-Galan et al., 2013) and subjects with MDD (Levine et al., 2000; Sanacora et al., 2004; Choudary et al., 2005; Njau et al., 2017). Intervention with antagonists to the NMDA receptor is efficient antidepressants in FSL/FRL rats and patients (Zarate Jr et al., 2006; Liebenberg et al., 2015; Silva et al., 2017). However, glutamate acts as an excitotoxic agent, inducing oxidative stress and damaged mitochondrial calcium homeostasis by disturbing the closely regulated balance between mitochondrial fission and fusion (Fukui et al., 2010; Nguyen et al., 2011), leading to mitochondrial dysfunction

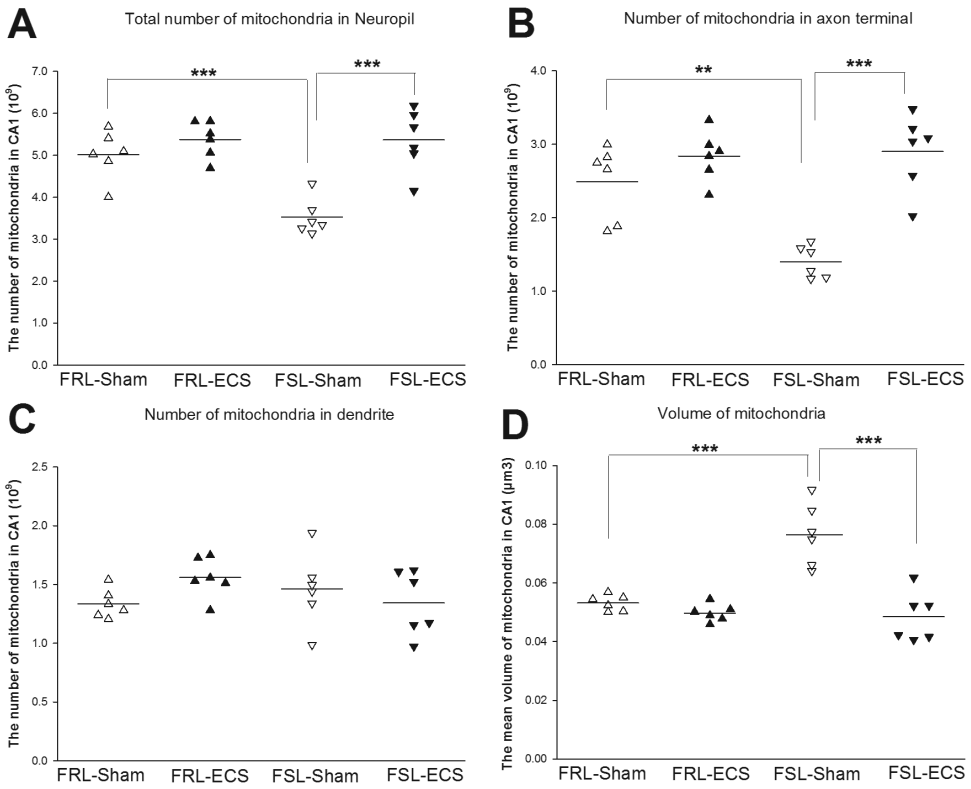

Figure 6. The number of mitochondria in the various structures (neuropil, axons, and dendrites) and the mean volume of mitochondria in CA1. (*P < .05; **P < .01; ***P < .001) (ΔFlinders Resistant Line (FRL)-Sham rats; ▲FRL-electroconvulsive seizure (ECS) rats; ▽Flinders Sensitive Line (FSL)-Sham rats; ▼FSL-ECS rats). (A) The total number of mitochondria in neuropil was significantly smaller in the FSL-sham group compared with FRL-sham group. Following treatment, the FSL-ECS group showed a significant increase in total mitochondria number in neuropil compared with the FSL-sham group. (B) The number of mitochondria in axon terminal also displayed significantly smaller in the FSL-sham group compared with the FRL-sham group. Following treatment, the FSL-ECS group showed a significant increase in mitochondria number in axon terminal compared with the FSL-sham group. (C) The number of mitochondria in dendrites showed no significant differences in the FSL sham group compared with the FRL sham group. ECS treatment did not make any changes in the number of mitochondria in dendrites between the FSL sham group and FSL ECS group. (D) The mean volume of mitochondria in CA1 stratum radiatum was significantly greater in the FSL-sham group compared with FRL-sham group. Following treatment, the mean volume of mitochondria in FSL-ECS group showed a significant increase compared with the FSL-sham group.

and swelling (Lemberg and Fernandez, 2009). We observed a larger mean volume of mitochondria in the FSL rats, which might be due to the increased glutaminergic synaptic activity inducing mitochondrial swelling. Furthermore, Li et al. have demonstrated that inhibition of mitochondrial fission in hippocampal neurons causes elongation of mitochondria (Li et al., 2004). It is interesting that the results showed no significant differences between the FSL and the FRL rats when we estimated the total volume of mitochondria in CA1 (Table 1). This seems to implicate that the fission-fusion balance of mitochondria is disturbed and shifts away from fission. However, whether mitochondrial dynamics is abnormal in these rats still needs more investigation, such as measuring expression of fusion and fission proteins. ECS has been documented decreasing glutamate levels in the hippocampus of subjects with MDD (Njau et al., 2017) by altered expression of glutamate signaling. This could be due to an increased glutamate receptor subtype (GluR1) (a subunit of the AMPA receptor) (Wong et al., 1993) and induction of the glutamine transporter GLT1 and the enzyme glutamine synthetase that converts glutamate to nontoxic glutamine (Newton et al., 2006), finally leading to prevention of glutamate excitotoxicity and recovery of mitochondrial volume.

Effect of ECS on Hippocampal BDNF Expression

Our present results showed that BDNF positive immunoreactivity in DG and CA areas of the hippocampus was significantly higher in both FSL-ECS and FRL-ECS rats compared with the sham rats. Postmortem study of the hippocampus showed increased levels of BDNF immunoreactivity in depressed patients treated with antidepressants at the time of death, compared with antidepressant-untreated subjects (Chen et al., 2001). More recently, it has been indicated that dysregulation of the activity-dependent neurotrophin BDNF resulted in disrupted glucocorticoid rhythms and tissue resistance to signaling with the glucocorticoid receptor as an important mechanism underlying stress-related neuropsychiatric disorders (Jeanneteau and Arango-Lievano, 2016). Our findings are consistent with their findings. However, BDNF immunoreactivity in our present study showed no differences between FRL-sham and FSL-sham rat. Similar results from Angelucci et al. (Angelucci et al., 2000, 2003) showed no difference in the BDNF levels measured by ELISA in the hippocampus of depressed FSL compared with FRL control rats. However, there are still some inconsistencies in the results compared with other studies using a genetic animal model of depression. BDNF was decreased at both the mRNA and protein level in FSL rats compared with FRL rats in the hippocampus (Elfving et al., 2010). The discrepancies may be explained by 2 reasons. First, the age of the animals in the present study was around 60 days vs 140 days in the previous reports. The levels of brain and serum BDNF in different time-slots has been reported to change during maturation and aging processes (Karege et al., 2002). Second, BDNF-positive areas in the present study were estimated in different subregions of hippocampus vs whole hippocampus in the previous studies.

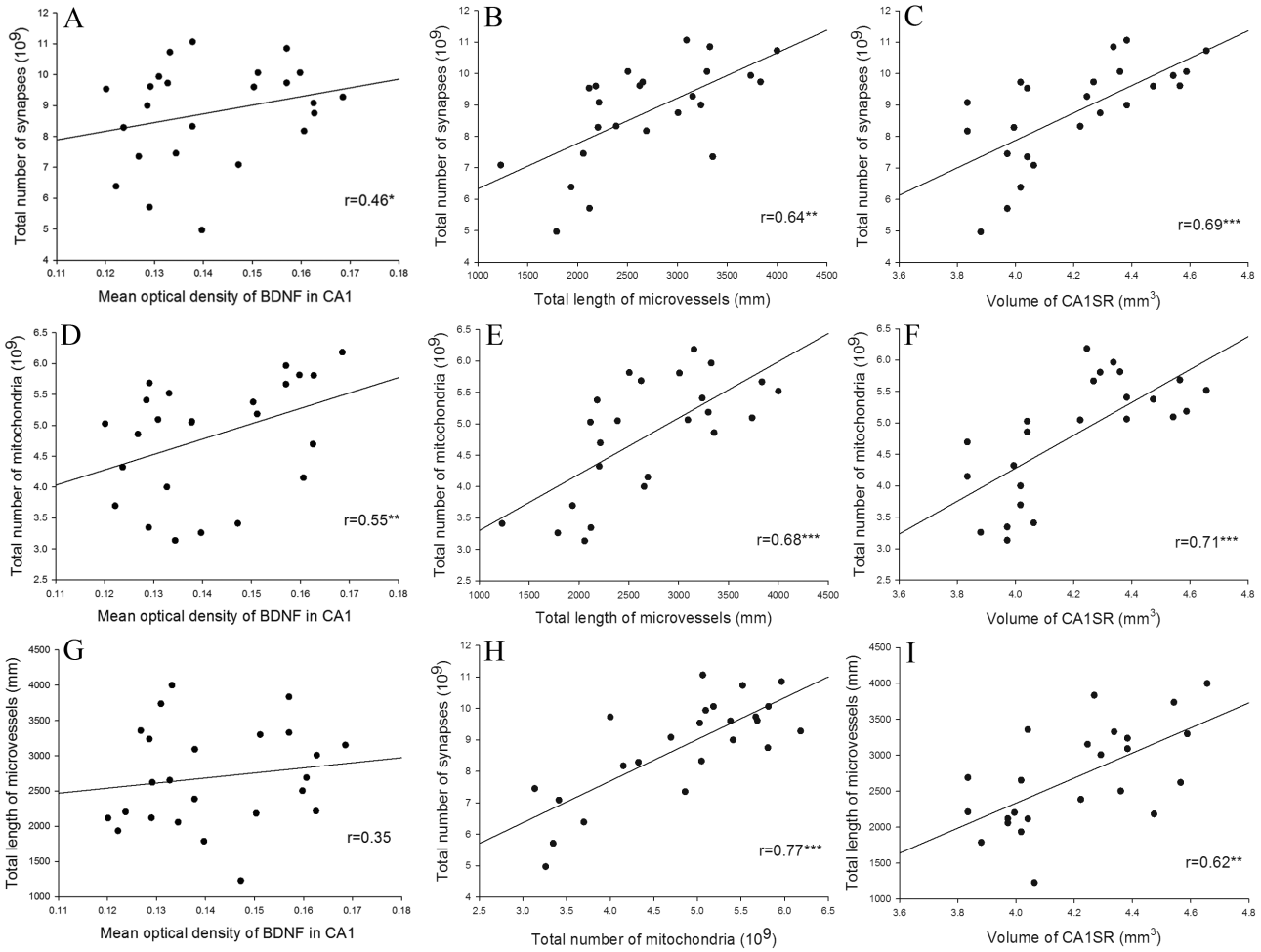

Figure 7. The correlations between synaptic plasticity and nonneuronal plasticity of hippocampus (*P < .05; **P < .01; ***P < .001). The levels of brain-derived neurotrophic factor (BDNF) expression correlated positively with synapse number (A) and mitochondrial number (D), but not the total length of microvessels (G). Total length of microvessels showed a significant positive correlation with synapse number (B) and mitochondrial number (E). In addition, the volume of hippocampal CA1-SR correlated positively with synapse number (C), mitochondrial number (F), and total length of microvessels (I). Furthermore, there was a significant positive correlation between the total mitochondria number density and total number of synapses (H).

Effect of ECS on Hippocampal Vascular Plasticity: Length of Microvessels

Earlier reports demonstrated that ECS-induced upregulation of angiogenic factors results in increased vascular density in hippocampus (Newton et al., 2006). The vascular endothelial growth factor and basic fibroblast growth factor possess both angiogenic as well as neurotrophic properties in hippocampus (Newton et al., 2003). Our findings showed decreased length of microvessels in the depressed FSL-sham rats compared with the FRL control rats. Increased length of microvessels in the FSL-ECS rats were in agreement with those observations above.

The Relationship between Synaptic Plasticity and Nonneuronal Plasticity of Hippocampus in Depression

Several lines of evidence suggest that neurotrophic factors serve as mediators of activity-dependent structural plasticity and play a key regulator of neuronal functioning (Bouckaert et al., 2014; Leal et al., 2015). BDNF promotes neuronal differentiation and survival and synaptic plasticity (Duman and Monteggia, 2006; Kermani and Hempstead, 2007). The consequence of the abnormality in the BDNF and GR signaling is impairment of mitochondrial respiration efficiency and synaptic plasticity (Jeanneteau and Arango-Lievano, 2016). The study about BNDF-induced mitochondrial motility arrest and presynaptic docking suggests that mitochondrial transport and distribution play an essential role in BDNF-mediated synaptic transmission (Su et al., 2014b). Our results also indicate that BDNF has a significant positive correlation with synapse and mitochondrial number.

Several studies suggest that physical proximity between mitochondria and synapses is regulated by neuronal activity (Courchet et al., 2013; Sheng, 2014). Enduring changes in metabolic support of brain function, such as modifications of capillary branching or mitochondrial density, have been primarily studied as problems of either development or pathology (Black et al., 1991). High levels of monocarboxylate (Gerhart et al., 1998) and glucose (Gerhart et al., 1991) transporters were observed in the CA1, suggesting elevated metabolic and synaptic activity in this region of the hippocampus. Our results showed that increased total synapse number is positively correlated with total mitochondria number. The mitochondrial changes may be crucially linked to changed energy metabolism and, therefore, may have consequences for cell plasticity, resilience, and survival in patients with MDD. Antidepressants might ultimately enhance energy metabolism and reduce the damage of oxidative stress.

Furthermore, our results demonstrate that increased supports higher metabolic demand due to an increase in the number of synapses and mitochondria.

Taken together, even though we have only investigated a portion of the hippocampus, our results indicate that the rapid and robust therapeutic effect of ECS may be related to BDNF level elevation, accompanied by synaptic plasticity, mitochondrial and vascular support. Moreover, the changes in mitochondrial morphology and number are a consistent feature of neuroplasticity, and therefore, the relation between synapses and mitochondria is a pivot for neuronal plasticity. Overall, this study provides insights into the underlying mechanisms of a rapid antidepressant effect.

Acknowledgments

We thank Nadia G. Knudsen and Linda Damgaard for their help in caring for and overseeing the experimental animals. Herdis Krunderup, Lone Lysgaard, and Anette Berg are gratefully acknowledged for their skillful EM technical assistance. We thank David H. Overstreet, University of North Carolina at Chapel Hill, North Carolina, for providing us with the initial FSL/FRL breeding pairs.

Statement of Interest

Dr Chen received research funding and salary support from the Danish Research Council and Lundbeck Foundation. Dr Ardalan had salary support from Lundbeck Foundation. Dr Elfving received research funding from the Danish Medical Research Council. Dr Madsen received research funding from the Danish Medical Research Council and Lundbeck Foundation and is a full-time employee and stockholder in Aptinyx, Inc. Dr Nyengaard received research funding from Sino-Danish Center and the Villum Foundation via Centre for Stochastic Geometry and Advanced Bioimaging. Dr Wegener received lecture/consultancy fees from H. Lundbeck A/S, Servier SA, Astra Zeneca AB, Eli Lilly A/S, Sun Pharma Pty Ltd, Pfizer Inc, Shire A/S, HB Pharma A/S, Arla Foods A.m.b.A., Alkermes Inc, and Mundipharma International Ltd., and research funding from the Danish Medical Research Council, Aarhus University Research Foundation (AU-IDEAS initiative (eMOOD)), the Novo Nordisk Foundation, the Lundbeck Foundation, and EU Horizon 2020 (ExEDE).

Conflict of Interest

None declared.

References

Angelucci F, Aloe L, Vasquez PJ, Mathe AA (2000) Mapping the differences in the brain concentration of brain-derived neurotrophic factor (BDNF) and nerve growth factor (NGF) in an animal model of depression. Neuroreport 11:1369–1373.

Angelucci F, Aloe L, Jimenez-Vasquez P, Mathe AA (2003) Electroconvulsive stimuli alter nerve growth factor but not brain-derived neurotrophic factor concentrations in brains of a rat model of depression. Neuropeptides 37:51–56.

Ardalan M, Wegener G, Polsinelli B, Madsen TM, Nyengaard JR (2016) Neurovascular plasticity of the hippocampus one week after a single dose of ketamine in genetic rat model of depression. Hippocampus 26:1414–1423.

Ardalan M, Wegener G, Rafati H, Nyengaard R (2017) S-Ketamine rapidly reverses synaptic and vascular deficits of hippocampus in genetic animal model of depression. Int J Neuropsychopharmacol 20:247–256.

Bae J, Sung BH, Cho IH, Song WK (2012) F-actin-dependent regulation of NESH dynamics in rat hippocampal neurons. PLoS One 7:e34514.

Black JE, Zelazny AM, Greenough WT (1991) Capillary and mitochondrial support of neural plasticity in adult rat visual cortex. Exp Neurol 111:204–209.

Boldrini M, Hen R, Underwood MD, Rosoklija GB, Dwork AJ, Mann JJ, et al (2012) Hippocampal angiogenesis and progenitor cell proliferation are increased with antidepressant use in major depression. Biol Psychiatry 72:562–571.

Bouckaert F, Sienaert P, Obbels J, Dols A, Vandenbulcke M, Stek M, et al (2014) ECT: its brain enabling effects: a review of electroconvulsive therapy–induced structural brain plasticity. J ECT 30:143–151.

Calverley RK, Jones DG (1990) Contributions of dendritic spines and perforated synapses to synaptic plasticity. Brain Res Brain Res Rev 15:215–249.

Cataldo AM, McPhie DL, Lange NT, Punzell S, Elmiligy S, Ye NZ, et al (2010) Abnormalities in mitochondrial structure in cells from patients with bipolar disorder. Am J Pathol 177:575–585.

Chan D, Frank S, Rojo M (2006) Mitochondrial dynamics in cell life and death. Cell Death Differ 13:680–684.

Chen B, Dowlatshahi D, MacQueen GM, Wang JF, Young LT (2001) Increased hippocampal BDNF immunoreactivity in subjects treated with antidepressant medication. Biol Psychiatry 50:260–265.

Chen F, Madsen TM, Wegener G, Nyengaard JR (2008) Changes in rat hippocampal CA1 synapses following imipramine treatment. Hippocampus 18:631–639.

Chen F, Madsen TM, Wegener G, Nyengaard JR (2009) Repeated electroconvulsive seizures increase the total number of synapses in adult male rat hippocampus. Eur Neuropsychopharmacol 19:329–338.

Chen F, Madsen TM, Wegener G, Nyengaard JR (2010) Imipramine treatment increases the number of hippocampal synapses and neurons in a genetic animal model of depression. Hippocampus 20:1376–1384.

Chen F, Wegener G, Madsen TM, Nyengaard JR (2013) Mitochondrial plasticity of the hippocampus in a genetic rat model of depression after antidepressant treatment. Synapse 67:127–134.

Chen H, Chan DC (2009) Mitochondrial dynamics-fusion, fission, movement, and mitophagy-in neurodegenerative diseases. Hum Mol Genet 18:R169–R176.

Cheng A, Hou Y, Mattson MP (2010) Mitochondria and neuroplasticity. ASN Neuro 2:e00045.

Choudary PV, Molnar M, Evans SJ, Tomita H, Li JZ, Vawter MP, et al (2005) Altered cortical glutamatergic and GABAergic signal transmission with glial involvement in depression. Proc Natl Acad Sci U S A 102:15653–15658.

Courchet J, Lewis TL Jr, Lee S, Courchet V, Liou DY, Aizawa S, et al (2013) Terminal axon branching is regulated by the LKB1–NUAK1 kinase pathway via presynaptic mitochondrial capture. Cell 153:1510–1525.

Czeh B, Abumaria N, Rygula R, Fuchs E (2010) Quantitative changes in hippocampal microvasculature of chronically stressed rats: no effect of fluoxetine treatment. Hippocampus 20:174–185.

Detmer SA, Chan DC (2007) Functions and dysfunctions of mitochondrial dynamics. Nat Rev Mol Cell Biol 8:870–879.

Dong WK, Greenough WT (2004) Plasticity of nonneuronal brain tissue: roles in developmental disorders. Ment Retard Dev Disabil Res Rev 10:85–90.

Duman JG, Tzeng CP, Tu YK, Munjal T, Schwechter B, Ho TS, et al (2013) The adhesion–GPCR BAI1 regulates synaptogenesis by controlling the recruitment of the Par3/Tiam1 polarity complex to synaptic sites. J Neurosci 33:6964–6978.

Duman RS (2004) Neural plasticity: consequences of stress and actions of antidepressant treatment. Dialogues Clin Neurosci 6:157–169.

Duman RS, Monteggia LM (2006) A neurotrophic model for stress–related mood disorders. Biol Psychiatry 59:1116–1127.

Ekemohn M, Kjaer NM, Grahm M, Tingstrom A, Kousholt B, Wegener G, et al (2017) Systematic evaluation of skeletal fractures caused by induction of electroconvulsive seizures in rat state a need for attention and refinement of the procedure. Acta Neuropsychiatr 29:363–373.

Elfving B, Plougmann PH, Muller HK, Mathe AA, Rosenberg R, Wegener G (2010) Inverse correlation of brain and blood BDNF levels in a genetic rat model of depression. Int J Neuropsychopharmacol 13:563–572.

Fukui M, Choi HJ, Zhu BT (2010) Mechanism for the protective effect of resveratrol against oxidative stress-induced neuronal death. Free Radic Biol Med 49:800–813.

Ganeshina O, Berry RW, Petralia RS, Nicholson DA, Geinisman Y (2004) Synapses with a segmented, completely partitioned postsynaptic density express more AMPA receptors than other axospinous synaptic junctions. Neuroscience 125:615–623.

Geinisman Y, Disterhoft JF, Gundersen HJ, McEchron MD, Persina IS, Power JM, et al (2000) Remodeling of hippocampal synapses after hippocampus-dependent associative learning. J Comp Neurol 417:49–59.

Geinisman Y, Berry RW, Disterhoft JF, Power JM, Van der Zee EA (2001) Associative learning elicits the formation of multiple-synapse boutons. J Neurosci 21:5568–5573.

Gerhart DZ, Djuricic B, Drewes LR (1991) Quantitative immunocytochemistry (image analysis) of glucose transporters in the normal and postischemic rodent hippocampus. J Cereb Blood Flow Metab 11:440–448.

Gerhart DZ, Enerson BE, Zhdankina OY, Leino RL, Drewes LR (1998) Expression of the monocarboxylate transporter MCT2 by rat brain glia. Glia 22:272–281.

Gomez–Galan M, De BD, Van EA, Smolders I, Lindskog M (2013) Dysfunctional astrocytic regulation of glutamate transmission in a rat model of depression. Mol Psychiatry 18:582–594.

Hajszan T, MacLusky NJ, Leranth C (2005) Short–term treatment with the antidepressant fluoxetine triggers pyramidal dendritic spine synapse formation in rat hippocampus. Eur J Neurosci 21:1299–1303.

Hajszan T, Dow A, Warner-Schmidt JL, Szigeti-Buck K, Sallam NL, Parducz A, et al (2009a) Remodeling of hippocampal spine synapses in the rat learned helplessness model of depression. Biol Psychiatry 65:392–400.

Hajszan T, Dow A, Warner-Schmidt JL, Szigeti-Buck K, Sallam NL, Parducz A, et al (2009b) Remodeling of hippocampal spine synapses in the rat learned helplessness model of depression. Biol Psychiatry 65:392–400.

Hajszan T, Szigeti-Buck K, Sallam NL, Bober J, Parducz A, Maclusky NJ, et al (2010) Effects of estradiol on learned helplessness and associated remodeling of hippocampal spine synapses in female rats. Biol Psychiatry 67:168–174.

Jeanneteau F, Arango-Lievano M (2016) Linking mitochondria to synapses: new insights for stress-related neuropsychiatric disorders. Neural Plast 2016:3985063.

Jiao S, Li Z (2011) Nonapoptotic function of BAD and BAX in long-term depression of synaptic transmission. Neuron 70:758–772.

Jonas EA (2013) Contributions of Bcl–xL to acute and long term changes in bioenergetics during neuronal plasticity. Biochim Biophys Acta 1842:1168–1178.

Kaae SS, Chen F, Wegener G, Madsen TM, Nyengaard JR (2012) Quantitative hippocampal structural changes following electroconvulsive seizure treatment in a rat model of depression. Synapse 66:667–676.

Kang HJ, Voleti B, Hajszan T, Rajkowska G, Stockmeier CA, Licznerski P, et al (2012) Decreased expression of synapse–related genes and loss of synapses in major depressive disorder. Nat Med 18:1413–1417.

Kang JS, Tian JH, Pan PY, Zald P, Li C, Deng C, et al (2008) Docking of axonal mitochondria by syntaphilin controls their mobility and affects short-term facilitation. Cell 132:137–148.

Karege F, Schwald M, Cisse M (2002) Postnatal developmental profile of brain-derived neurotrophic factor in rat brain and platelets. Neurosci Lett 328:261–264.

Kermani P, Hempstead B (2007) Brain-derived neurotrophic factor: a newly described mediator of angiogenesis. Trends Cardiovasc Med 17:140–143.

Kodama M, Fujioka T, Duman RS (2004) Chronic olanzapine or fluoxetine administration increases cell proliferation in hippocampus and prefrontal cortex of adult rat. Biol Psychiatry 56:570–580.

Kovacevic T, Skelin I, Minuzzi L, Rosa-Neto P, Diksic M (2012) Reduced metabotropic glutamate receptor 5 in the flinders sensitive line of rats, an animal model of depression: an autoradiographic study. Brain Res Bull 87:406–412.

Kroustrup JP, Gundersen HJ (2001) Estimating the number of complex particles using the ConnEulor principle. J Microsc 203:314–320.

Larsen JO, Gundersen HJ, Nielsen J (1998) Global spatial sampling with isotropic virtual planes: estimators of length density and total length in thick, arbitrarily orientated sections. J Microsc 191:238–248.

Leal G, Afonso PM, Salazar IL, Duarte CB (2015) Regulation of hippocampal synaptic plasticity by BDNF. Brain Res 1621:82–101.

Lemberg A, Fernandez MA (2009) Hepatic encephalopathy, ammonia, glutamate, glutamine and oxidative stress. Ann Hepatol 8:95–102.

Levine J, Panchalingam K, Rapoport A, Gershon S, McClure RJ, Pettegrew JW (2000) Increased cerebrospinal fluid glutamine levels in depressed patients. Biol Psychiatry 47:586–593.

Li N, Lee B, Liu RJ, Banasr M, Dwyer JM, Iwata M, et al (2010a) mTOR–dependent synapse formation underlies the rapid antidepressant effects of NMDA antagonists. Science 329:959–964.

Li N, Liu RJ, Dwyer JM, Banasr M, Lee B, Son H, et al (2011) Glutamate N-methyl-D-aspartate receptor antagonists rapidly reverse behavioral and synaptic deficits caused by chronic stress exposure. Biol Psychiatry 69:754–761.

Li Z, Jo J, Jia JM, Lo SC, Whitcomb DJ, Jiao S, et al (2010b) Caspase-3 activation via mitochondria is required for long-term depression and AMPA receptor internalization. Cell 141:859–871.

Li Z, Okamoto K, Hayashi Y, Sheng M (2004) The importance of dendritic mitochondria in the morphogenesis and plasticity of spines and synapses. Cell 119:873–887.

Liebenberg N, Joca S, Wegener G (2015) Nitric oxide involvement in the antidepressant-like effect of ketamine in the Flinders sensitive line rat model of depression. Acta Neuropsychiatr 27:90–96.

MacAskill AF, Atkin TA, Kittler JT (2010) Mitochondrial trafficking and the provision of energy and calcium buffering at excitatory synapses. Eur J Neurosci 32:231–240.

MacAskill AF, Kittler JT (2010) Control of mitochondrial transport and localization in neurons. Trends Cell Biol 20:102–112.

Marcussen AB, Flagstad P, Kristjansen PE, Johansen FF, Englund U (2008) Increase in neurogenesis and behavioural benefit after chronic fluoxetine treatment in Wistar rats. Acta Neurol Scand 117:94–100.

Matrisciano F, Caruso A, Orlando R, Marchiafava M, Bruno V, Battaglia G, et al (2008) Defective group-II metaboropic glutamate receptors in the hippocampus of spontaneously depressed rats. Neuropharmacology 55:525–531.

Mattson MP, Pedersen WA, Duan W, Culmsee C, Camandola S (1999) Cellular and molecular mechanisms underlying perturbed energy metabolism and neuronal degeneration in Alzheimer's and Parkinson's diseases. Ann N Y Acad Sci 893:154–175.

Mattson MP, Gleichmann M, Cheng A (2008) Mitochondria in neuroplasticity and neurological disorders. Neuron 60:748–766.

Newton SS, Collier EF, Hunsberger J, Adams D, Terwilliger R, Selvanayagam E, et al (2003) Gene profile of electroconvulsive seizures: induction of neurotrophic and angiogenic factors. J Neurosci 23:10841–10851.

Newton SS, Girgenti MJ, Collier EF, Duman RS (2006) Electroconvulsive seizure increases adult hippocampal angiogenesis in rats. Eur J Neurosci 24:819–828.

Nguyen D, Alavi MV, Kim KY, Kang T, Scott RT, Noh YH, et al (2011) A new vicious cycle involving glutamate excitotoxicity, oxidative stress and mitochondrial dynamics. Cell Death Dis 2:e240.

Nicholson DA, Geinisman Y (2009) Axospinous synaptic subtype–specific differences in structure, size, ionotropic receptor expression, and connectivity in apical dendritic regions of rat hippocampal CA1 pyramidal neurons. J Comp Neurol 512:399–418.

Njau S, Joshi SH, Espinoza R, Leaver AM, Vasavada M, Marquina A, et al (2017) Neurochemical correlates of rapid treatment response to electroconvulsive therapy in patients with major depression. J Psychiatry Neurosci 42:6–16.

Obashi K, Okabe S (2013) Regulation of mitochondrial dynamics and distribution by synapse position and neuronal activity in the axon. Eur J Neurosci 38:2350–2363.

Overly CC, Rieff HI, Hollenbeck PJ (1996) Organelle motility and metabolism in axons vs dendrites of cultured hippocampal neurons. J Cell Sci 109:971–980.

Overstreet DH, Friedman E, Mathe AA, Yadid G (2005) The flinders sensitive line rat: a selectively bred putative animal model of depression. Neurosci Biobehav Rev 29:739–759.

Palmer CS, Osellame LD, Stojanovski D, Ryan MT (2011) The regulation of mitochondrial morphology: intricate mechanisms and dynamic machinery. Cell Signal 23:1534–1545.

Pittenger C, Duman RS (2008) Stress, depression, and neuroplasticity: a convergence of mechanisms. Neuropsychopharmacology 33:88–109.

Popoli M, Gennarelli M, Racagni G (2002) Modulation of synaptic plasticity by stress and antidepressants. Bipolar Disord 4:166–182.

Popov VI, Davies HA, Rogachevsky VV, Patrushev IV, Errington ML, Gabbott PL, et al (2004) Remodelling of synaptic morphology but unchanged synaptic density during late phase long-term potentiation (LTP) a serial section electron micrograph study in the dentate gyrus in the anaesthetised rat. Neuroscience 128:251–262.

Porsolt RD, Anton G, Blavet N, Jalfre M (1978) Behavioural despair in rats: a new model sensitive to antidepressant treatments. Eur J Pharmacol 47:379–391.

Reilly JE, Hanson HH, Phillips GR (2011) Persistence of excitatory shaft synapses adjacent to newly emerged dendritic protrusions. Mol Cell Neurosci 48:129–136.

Ren J, Li H, Palaniyappan L, Liu H, Wang J, Li C, et al (2014) Repetitive transcranial magnetic stimulation vs electroconvulsive therapy for major depression: a systematic review and meta–analysis. Prog Neuropsychopharmacol Biol Psychiatry 51:181–189.

Ruthel G, Hollenbeck PJ (2003) Response of mitochondrial traffic to axon determination and differential branch growth. J Neurosci 23:8618–8624.

Sanacora G, Gueorguieva R, Epperson CN, Wu YT, Appel M, Rothman DL, et al (2004) Subtype–specific alterations of gamma–aminobutyric acid and glutamate in patients with major depression. Arch Gen Psychiatry 61:705–713.

Scaglia F (2010) The role of mitochondrial dysfunction in psychiatric disease. Dev Disabil Res Rev 16:136–143.

Shao L, Martin MV, Watson SJ, Schatzberg A, Akil H, Myers RM, et al (2008) Mitochondrial involvement in psychiatric disorders. Ann Med 40:281–295.

Shao L, Vawter MP (2008) Shared gene expression alterations in schizophrenia and bipolar disorder. Biol Psychiatry 64:89–97.

Sheng ZH (2014) Mitochondrial trafficking and anchoring in neurons: new insight and implications. J Cell Biol 204:1087–1098.

Silva PV, Elfving B, Joca SRL, Wegener G (2017) Ketamine and aminoguanidine differentially affect Bdnf and Mtor gene expression in the prefrontal cortex of adult male rats. Eur J Pharmacol 815:304–311.

Small JV (1968) Measurement of section thickness, pp 609–610.

Sorra KE, Fiala JC, Harris KM (1998) Critical assessment of the involvement of perforations, spinules, and spine branching in hippocampal synapse formation. J Comp Neurol 398:225–240.

Stephenson JR, Paavola KJ, Schaefer SA, Kaur B, Van Meir EG, Hall RA (2013) Brain-specific angiogenesis inhibitor-1 signaling, regulation, and enrichment in the postsynaptic density. J Biol Chem 288:22248–22256.

Sterio DC (1984) The unbiased estimation of number and sizes of arbitrary particles using the disector. J Microsc 134:127–136.

Su B, Ji YS, Sun XL, Liu XH, Chen ZY (2014a) Brain-derived neurotrophic factor (BDNF)-induced mitochondrial motility arrest and presynaptic docking contribute to BDNF-enhanced synaptic transmission. J Biol Chem 289:1213–1226.

Su B, Ji YS, Sun XL, Liu XH, Chen ZY (2014b) Brain-derived neurotrophic factor (BDNF)-induced mitochondrial motility arrest and presynaptic docking contribute to BDNF-enhanced synaptic transmission. J Biol Chem 289:1213–1226.

Sun T, Qiao H, Pan PY, Chen Y, Sheng ZH (2013) Motile axonal mitochondria contribute to the variability of presynaptic strength. Cell Rep 4:413–419.

Tang Y, Nyengaard JR, De Groot DM, Gundersen HJ (2001) Total regional and global number of synapses in the human brain neocortex. Synapse 41:258–273.

Toni N, Buchs PA, Nikonenko I, Povilaitite P, Parisi L, Muller D (2001) Remodeling of synaptic membranes after induction of long-term potentiation. J Neurosci 21:6245–6251.

van SM, Mikhaylova M, Lipka J, Schlager MA, van den Heuvel DJ, Kuijpers M, et al (2013) TRAK/Milton motor-adaptor proteins steer mitochondrial trafficking to axons and dendrites. Neuron 77:485–502.

Vose LR, Stanton PK (2017) Synaptic plasticity, metaplasticity and depression. Curr Neuropharmacol 15:71–86.

Westermann B (2010) Mitochondrial fusion and fission in cell life and death. Nat Rev Mol Cell Biol 11:872–884.

Wong ML, Smith MA, Licinio J, Doi SQ, Weiss SR, Post RM, et al (1993) Differential effects of kindled and electrically induced seizures on a glutamate receptor (GluR1) gene expression. Epilepsy Res 14:221–227.

Yoshii A, Constantine-Paton M (2010) Postsynaptic BDNF-TrkB signaling in synapse maturation, plasticity, and disease. Dev Neurobiol 70:304–322.

Zarate CA Jr, Singh JB, Carlson PJ, Brutsche NE, Ameli R, Luckenbaugh DA, et al (2006) A randomized trial of an N-methyl-D-aspartate antagonist in treatment-resistant major depression. Arch Gen Psychiatry 63:856–864.

Zinsmaier KE, Babic M, Russo GJ (2009) Mitochondrial transport dynamics in axons and dendrites. Results Probl Cell Differ 48:107–139.